ACS APPLIED MATERIALS & INTERFACES

Research Article

www.acsami.org

# Forced Solid-State Interactions for the Selective "Turn-On" Fluorescence Sensing of Aluminum Ions in Water Using a Sensory Polymer Substrate

Saúl Vallejos, Asunción Muñoz, Saturnino Ibeas, Felipe Serna, Félix Clemente García, and José Miguel García*

Departamento de Química, Facultad de Ciencias, Universidad de Burgos, Plaza de Misael Bañuelos s/n, 09001 Burgos, Spain

Supporting Information

**ABSTRACT:** Selective and sensitive solid sensory substrates for detecting Al(III) in pure water are reported. The material is a flexible polymer film that can be handled and exhibits gel behavior and membrane performance. The film features a chemically anchored salicylaldehyde benzoylhydrazone derivative as an aluminum ion fluorescence sensor. A novel procedure for measuring Al(III) at the ppb level using a single solution drop in 20 min was developed. In this procedure, a drop was allowed to enter the hydrophilic material for 15 min before a 5 min drying period. The process forced the Al(III) to interact with the sensory motifs within the membrane before measuring the fluorescence of the system. The limit of detection of Al(III) was 22 ppm. Furthermore, a water-soluble sensory polymer containing the same sensory motifs was developed with a limit of detection of Al(III) of 1.5 ppb, which was significantly lower than the Environmental Protection Agency recommendations for drinking water.

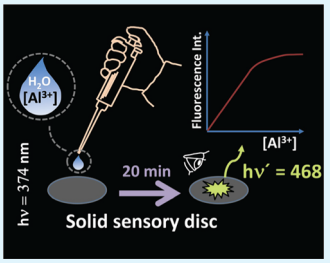


**KEYWORDS:** *sensory polymer, aluminum sensing, fluorescence chemosensor, fluorescence turn-on*

## INTRODUCTION

Aluminum is ubiquitous in nature, is the most abundant metallic element in the Earth's crust, and occurs in our everyday lives in metallic, alloy, and trivalent ion derivative forms. In fact, the importance of aluminum to humans is evidenced by its use as a preservative in food and drugs and as an additive in personal hygiene products, housewares, and technological devices. However, despite the tremendous impacts of aluminum on the socioeconomic development of mankind, the extensive application of aluminum results in environmental hazards, including the acidification of soils and aqueous media and toxicity toward aquatic biota.[1−3] Furthermore, aluminum presents an important health concern for humans because it is believed to be a causative factor for Alzheimer's and other diseases, such as dementia, encephalopathy, Parkinson's disease, and different types of cancer.[4−14]

Accordingly, detection and quantification devices for Al(III) are needed to mitigate medical and environmental risks, especially devices that could perform measurements cheaply, in situ, and in real time. On the basis of these considerations, optical chemosensors could play a vital role in developing these devices. However, few optical chemosensory systems based on the sensitive fluorescence technique have been reported,[15−27] and even fewer systems have been reported for sensing in pure water (the main medium of interest).[28−30]

Thus, we report a water-soluble polymer chemosensor that exhibits fluorescence "turn-on" for Al(III). Moreover, we describe a chemosensing polymer film substrate for the fluorescence detection and quantification of Al(III) and a new methodology for quantifying Al(III) within minutes at the ppb level that only uses a few microliters of the solution to be measured. Specifically, a drop of water containing Al(III) is absorbed by the solid hydrophilic sensory material. The absorption forces the solvated cations into the film, and the water is evaporated by applying heat. Consequently, the bare cations are forced to interact with the sensing motifs in the polymer structure, which increases the sensitivity and dramatically decreases the response time. The sensory materials were prepared through the copolymerization of a hydrophilic acrylic monomer with a novel methacrylic monomer featuring a salicylaldehyde benzoylhydrazone moiety as a sensing core for Al(III).

## EXPERIMENTAL SECTION

**Materials.** All materials and solvents were commercially available and used as received unless otherwise indicated. The following materials and solvents were obtained: 2,2-dimethoxy-2-phenylacetophenone (Aldrich, 99%), 2,2′-azobis(2-methylpropionitrile) (**AIBN**) (Aldrich, 98%), hydrazine monohydrate (Aldrich, 98%), 1-(4-aminophenyl)-1-propanone (Aldrich, 99%), ethanol absolute (VWR, 99.97%), salicylaldehyde (Merck, >99%), triethylamine (Aldrich, >99%), methacryloyl chloride (Alfa Aesar, 97%), 1-vinyl-2-pyrrolidone (**VP**) (Aldrich, 99%), 2-hydroxyethyl acrylate (**2HEA**) (Aldrich, 96%), ethylene glycol dimethacrylate (**EGDMMA**) (Aldrich, 98%), aluminum nitrate nonahydrate (Aldrich, 98%), ammonium nitrate (Aldrich, 98%), barium chloride dehydrate (LabKem, 99%), cadmium nitrate tetrahydrate (Alfa Aesar, 98.5%), cerium(III) nitrate hexahydrate (Alfa

Received: October 28, 2014
Accepted: December 5, 2014
Published: December 5, 2014

  

Aesar, 99.5%), cesium nitrate (Fluka, 99%), cobalt(II) nitrate hexahydrate (LabKem, 98%), copper(II) nitrate trihydrate (Aldrich, 98%), dysprosium(III) nitrate hydrate (Alfa Aesar, 99.9%), iron(II) sulfate heptahydrate (Aldrich, 99%), iron(III) nitrate nonahydrate (Aldrich, 98%), lanthanum(III) nitrate hexahydrate (Alfa Aesar, 99.9%), lead(II) nitrate (Fluka, 99%), lithium chloride (Aldrich, 99%), magnesium nitrate hexahydrate (LabKem, 98%), manganese(II) nitrate hexahydrate (Alfa Aesar, 98%), mercury(II) nitrate monohydrate (Scharlab, 99%), neodymium(III) nitrate hexahydrate (Alfa Aesar, 99.9%), nickel(II) nitrate hexahydrate (VWR, 99%), platinum(II) chloride (Aldrich, 98%), chromium(III) nitrate nonahydrate (Alfa Aesar, 98.5%), potassium dichromate (Aldrich, 99.5%), potassium nitrate (Aldrich, 99%), rubidium nitrate (Aldrich, 99.7%), samarium(III) nitrate hexahydrate (Alfa Aesar, 99.9%), silver nitrate (LabKem, 99%), sodium nitrate (LabKem, 99%), strontium nitrate (Alfa Aesar, 98%), tin(II) chloride (Aldrich, 98%), zinc nitrate hexahydrate (Aldrich, 98%), zirconium(IV) chloride (Alfa Aesar, 98%), *N*,*N*-dimethylformamide (DMF) (Aldrich, 99.9%), and *N*,*N*-dimethylacetamide (DMA) (Merck, 99%).

**Measurements and Instrumentation.** The $^{27}$Al, $^{1}$H, and $^{13}$C NMR spectra were recorded with a Varian Inova 400 spectrometer operating at 104.21, 399.92, and 100.57 MHz with deuterated dimethyl sulfoxide (DMSO-$d_6$), deuterium oxide ($D_2O$), or a 80:20 mixture of both, respectively, as the solvents. The fluorescence spectra were recorded using an F-7000 Hitachi Fluorescence spectrophotometer. Thermogravimetric analysis (TGA) data were recorded using 4−5 mg of sample under a synthetic air atmosphere with a TA Instruments Q50 TGA analyzer at 10 °C min$^{-1}$. In addition, IR-ATR infrared spectra (FTIR) were recorded using a JASCO FT/IR-4100 fit with a PIKE TECH "Miracle" ATR accessory.

Gel permeation chromatography (GPC) analysis was conducted using PSS-GRAM columns with nominal pore sizes of 30, 100, and 3000 Å. For this analysis, *N*,*N*-dimethylformamide (DMF)/0.01 M LiBr was used as the solvent, and the measurements were performed at 70 °C at a flow rate of 1.0 mL/min and by using an RI detector. The columns were calibrated using narrow distribution standards of poly(methyl methacrylate).

Scanning electron microscopy (SEM) images were obtained from the gold-sputtered membranes using a JEOL JSM-6460LV instrument with an Oxford Instruments INCA EDS (energy-dispersive X-ray spectroscopy). The membrane cross section was obtained after breaking the material cryogenically in liquid nitrogen.

Al(III) titration experiments were conducted with the sensory monomer (**3**) and sensory linear polymer ($\mathbf{L}_{Sen}$) as follows. Solutions of (**3**) ($2 \times 10^{-3}$ M in DMA/water, 50/50) and $\mathbf{L}_{Sen}$ (0.25 mEq/L of sensory motifs) in Millipore-Q water (pH = 4.5, buffered with NaOH/AcOH) were prepared and transferred to the cuvette used for measurement. The concentration of Al(III) was progressively increased by adding cumulative volumes of $1 \times 10^{-10}$ to $1 \times 10^{-1}$ M aqueous stock (Millipore-Q, pH = 4.5) solutions containing $Al(NO_3)_3{\cdot}9H_2O$. Fluorescence spectra were captured 5 min after each addition.

The Al(III) titration experiments using the sensory membrane ($\mathbf{M}_{Sem}$) were carried out as follows. First, 5 $\mu$L of the Al(III) solutions in Millipore-Q water (pH = 4.5, buffered with NaOH/AcOH with an Al(III) concentration ranging from 56 ppb to 5600 ppm) were deposited on the surfaces of sensory discs and allowed to stand for 15 min. Next, the samples were heated for 5 min at 100 °C before being allowed to cool to room temperature (rt) for 10 min. The fluorescence intensities were then measured by positioning the membrane vertically in the spectrofluorometer and at 45° with respect to the light source and the detector. Thus, the reflection of the source light on the film surface was prevented from reaching the detector by placing the discs in a position where the source light would hit the discs on one side; the other side would emit the detected light, with the reflected light going in the opposite direction.

The high-resolution mass spectrometry (HRMS) data were obtained in an API QSTAR XL Hybrid spectrometry system (Applied Biosystems) using an electrospray ionization (ESI) with a high resolution or a fast atom bombardment (FAB) with DMSO as solvent. The quantum yields ($\Phi$) were measured in DMA using quinine sulfate in sulfuric acid (0.05 M) as a reference standard.[31] The water-swelling percentage (WSP), which is the weight percentage of water taken up by the films after soaking and until equilibrium was reached, in pure water was calculated based on the weights of a dry sample film ($w_d$) and a water-swelled sample film ($w_s$) (the membranes were immersed in pure water at 20 °C until the swelling equilibrium was achieved) as follows: $100[(w_s - w_d)/w_d]$. The mechanical properties of the membranes were measured using a Shimadzu EZ Test Compact Table-Top Universal Tester at 20 °C.

**Monomer Synthesis.** The methacrylamide monomer (*E*)-*N*-(4-(2-(2-hydroxybenzylidene)hydrazine-carbonyl)phenyl) methacrylamide (**3**) was synthesized from inexpensive and readily available chemicals using proven and high-yield organic reactions, beginning with ethyl 4-aminobenzoate. Details regarding the synthesis process are described below and are schematically depicted in Scheme 1.

**Scheme 1. Monomer (3) Synthesis and Structure**

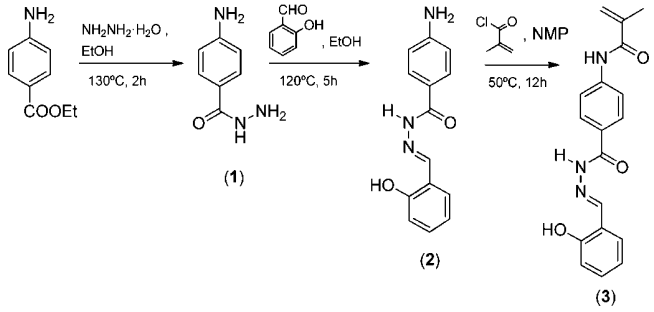


**Intermediate Synthesis.** *4-Aminobenzohydrazide (**1**).* First, 72 mL (1.5 mol) of hydrazine monohydrate and 20 g (121 mmol) of ethyl 4-aminobenzoate were added to a 500 mL pressure tube that was fit with a magnetic stirrer. The solution was stirred at 130 °C for 45 min and cooled to rt. Next, 130 mL of absolute ethanol was added, and the solution was stirred at 100 °C for 1 h. Finally, the solution was cooled and filtered, and the product was washed with water (the product was recrystallized in ethanol). Yield (after recrystallization): 12 g (65%). $^{1}$H NMR (399.94 MHz; DMSO-$d_6$): $\delta$ (ppm), 9.41 (s, 1H); 7.66 (d, 2H, 8.6 Hz); 7.64 (d, 2H, 8.6 Hz); 5.64 (s, 2H); 4.44 (s, 2H). $^{13}$C NMR (100.58 MHz; DMSO-$d_6$): $\delta$ (ppm), 167.78, 152.61, 129.60, 121.07, and 113.84. Electron impact mass spectrometry (EI-MS), *m*/*z*: 151 ($M^+$, 7), 121 (7), 120 (100), 93 (5), 92 (54), 91 (5), 78 (11), 69 (6), 65 (34), and 63 (14). FTIR (wavenumber, cm$^{-1}$): $\nu_{NH}$ 3427, 3345, 3300, and 3236; $\nu_{C=O}$: 1660. ESI-HRMS calcd for $C_{18}H_{17}N_3O_3$ 151.0746, found 151.0745.

*(E)-4-amino-N′-(2-hydroxybenzylidene)benzohydrazide (**2**).* First, 1 g (6 mmol) of compound (**1**), 803 mg (6 mmol) of salicylaldehyde, and 20 mL of ethanol were added to a 100 mL pressure tube. The mixture was stirred at 120 °C for 5 h. Next, the reaction was allowed to occur at rt, and a pale-yellow precipitate was filtered off and washed with a small amount of cool ethanol. Yield: 1.32 g (86%). $^{1}$H NMR (399.94 MHz; DMSO-$d_6$): $\delta$ (ppm), 11.69 (s, 1H), 8.60 (s, 1H), 7.74 (d, 2H, 8.60 Hz), 7.51 (dd, 1H, 7.6 and 1.3 Hz), 7.34−7.28 (m, 1H), 6.99−6.91 (m, 2H), 6.66 (d, 2H, and 8.7 Hz), and 5.88 (s, 1H). $^{13}$C NMR (100.58 MHz; DMSO-$d_6$): $\delta$ (ppm), 163.58, 158.36, 153.48, 147.84, 131.82, 130.58, 130.34, 120.13, 119.69, 119.66, 117.31, and 113.59. EI-MS, *m*/*z*: 255 ($M^+$, 9.14), 151 (5), 136 (7), 121 (8), 120 (100), 92 (19), 78 (10), 65 (12), and 63 (10). FTIR (wavenumber, cm$^{-1}$): $\nu_{OH,\ NH}$ 3455, 3356, and 3281; $\nu_{C=O}$: 1664. ESI-HRMS calcd for $C_{18}H_{17}N_3O_3$ 255.1008, found 255.1008.

**Monomer Synthesis.** *(E)-N-(4-(2-(2-Hydroxybenzylidene)-hydrazinecarbonyl)phenyl) methacrylamide (**3**).* First, 1.55 mmol (0.5 g) of product (**2**), 2.32 mmol (0,324 mL) of triethylamine, and 15 mL of NMP were added to a pressure tube. Subsequently, 2.01 mmol (0,197 mL) of methacryloyl chloride was added to the tube, and the solution was stirred for 12 h at 50 °C under a nitrogen atmosphere. Finally, the solution was added to water, and the product (**3**) was

**Scheme 2. Monomer, Linear Copolymer ($L_{Sen}$), and Membrane ($M_{Sen}$) Structures**[a]

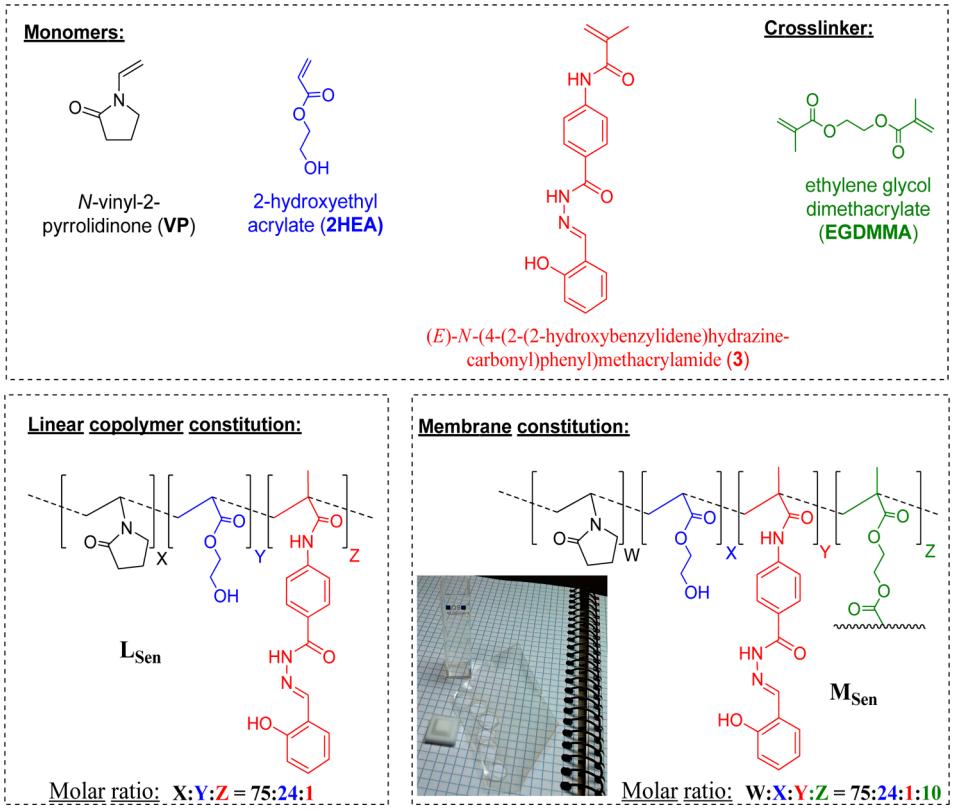


[a]The photograph of the membrane on a notebook shows the aspect ratio and the transparency of the sensory material; the holes correspond to the areas where the 5 mm discs were removed for the sensory kits.

filtered and recrystallized in ethanol. Yield: 0.35 g (70%). $^1$H NMR (399.94 MHz; DMSO-$d_6$): $\delta$ (ppm), 12.08 (s, 1H), 11.40(s, 1H), 10.11 (s, 1H), 8.68 (s, 1H), 7.97 (d, 2H, and 8.3 Hz), 7.90 (d, 2H, and 8.0 Hz), 7.57 (d, 1H, and 7.6 Hz), 7.34 (t, 1H, and 7.7 Hz), 7.02−6.92 (m, 2H), 5.90 (s, 1H), 5.62 (s, 1H), and 2.01 (s, 3H). $^{13}$C NMR (100.58 MHz; DMSO-$d_6$): $\delta$ (ppm), 168.03, 163.16, 158.39, 148.90, 143.39, 141.09, 132.20, 130.50, 129.33, 128.14, 121.51, 120.29, 120.25, 119.62, 117.34, and 19.60. EI-MS, $m/z$: 323 ($M^+$, 17), 204 (15), 189 (14), 188 (100), 121 (17), 120 (7), and 69 (9). IR (wavenumber, cm$^{-1}$): $\nu_{OH,\ NH}$: 3450 (bb), 3320 and 3251; $\nu_{C=O}$: 166. ESI-HRMS calcd for $C_{18}H_{17}N_3O_3$ 323.1270, found 323.1267.

*Al(III)-((E)-N-(4-(2-(2-Hydroxybenzylidene)hydrazinecarbonyl)-phenyl)) complex ($C_{1:3}$).* First, 253 mg (0.782 mmol) of the monomer (**3**), 98 mg (0.261 mmol) of aluminum nitrate nonahydrate, and 25 mL of ethanol were added to a 100 mL pressure tube. Next, the mixture was stirred at 120 °C for 5 h and overnight at 50 °C. The solvent was removed under vacuum, and the yellow solid product was washed with water. Yield: 45%. $^{27}$Al NMR (104.23 MHz; DMSO-$d_6$): $\delta$ (ppm), 18.48, and 11.75. HR-ESI-MS, $m/z$: 324.1367 [(**3**) + H]$^+$ (calcd for $C_{18}H_{18}N_3O_3$, 324.1348), 671.2243 [Al(**3**)$_2$]$^+$ (calcd for $C_{36}H_{32}AlN_6O_6$, 671.2199), 994.3458 [$C_{1:3}$ + H]$^+$ (calcd for $C_{54}H_{49}AlN_9O_9$, 994.3469), and 1016.3298 [$C_{1:3}$ + Na]$^+$ (calcd for $C_{54}H_{48}AlN_9O_9Na$, 1016.3288). Anal. Calcd (found) for $C_{1:3}$: C 65.25 (65.16), H 4.87 (4.85), and N 12.68 (12.83)%.

**Material Preparation.** *Linear Copolymer Synthesis.* The linear copolymer ($L_{Sen}$) was prepared by the photochemically initiated free radical polymerization of the **VP** and **2HEA** hydrophilic monomers and the sensing monomer (**3**) at a **VP**/**2HEA**/(**3**) molar ratio of 74.5:24.5:1.0.

A 100 mL three-neck flask equipped with a magnetic stirrer and a reflux condenser was blanketed with nitrogen through a gas inlet. Then, 0.37 mmol (120 mg) of (**3**), 27.32 mmol (3.04 g) of **VP**, and 9.10 mmol (1.06 g) of **2HEA** were dissolved in DMF (37 mL) and added to the flask. Subsequently, 2,2-dimethoxy-2-phenylacetophenone (948 mg, 3.70 mmol) was added to the flask, and the solution was irradiated for 12 h at rt (250 w UV mercury lamp, Philips HPL-N, emission bands in the UV region at 304, 314, 335, and 366 nm with the maximum emission at 366 nm). The resulting solution was added dropwise to diethyl ether (300 mL) while vigorously stirring to yield a brown precipitate. The polymer was purified using two cycles of a solution/precipitation procedure with methanol (10 mL) as the solvent and diethyl ether (100 mL) as the nonsolvent. Finally, the solution was dried overnight in a vacuum oven at 60 °C (resulting in a yield of 3.60 g (85%)). The mass average molar mass ($M_w$) was 12.4 × 10$^4$ Da.

*Membrane Preparation.* The cross-linked film or membrane ($M_{Sen}$) was prepared by thermally initiated bulk free radical polymerization with **VP**, **2HEA**, (**3**), and **EGDMMA** as a cross-linking agent at a comonomer molar ratio of 74/25/1/10 (**VP**/**2HEA**/(**3**)/**EGDMMA**) and using **AIBN** (1 wt %) as the thermal radical initiator. The homogeneous solution of comonomers was transferred to an ampule, degassed by bubbling the solution with nitrogen for 15 min, injected into a 200 $\mu$m thick silanized glass hermetic mold in an oxygen-free environment, and heated to 60 °C for 12 h. Next, the membrane was demolded and conditioned by allowing it to stand for 24 h at rt. The chemical structure is depicted in Scheme 2.

*Hybrid Membrane Preparation (Al-$M_{Sen}$).* A hybrid Al(III)-$M_{Sen}$ membrane (**Al-M$_{Sen}$**) was prepared by immersing $M_{Sen}$ in a 0.1 M aluminum nitrate nonahydrate solution at pH 2 for 2 h. Next, it was thoroughly washed with water and acetone and dried under ambient conditions for 48 h.

## RESULTS AND DISCUSSION

To improve the performance of chemosensors, we addressed the task of designing a material that can be handled and exhibits improved fluorescence "off−on" sensing capabilities for Al(III). Thus, we synthesized a novel methacrylic monomer featuring a

salicylaldehyde hydrazone moiety as the sensing core for Al(III) (Scheme 1).

This monomer was used to prepare solid sensory films ($\mathbf{M}_{Sen}$). In addition, this monomer was used to synthesize a water-soluble sensory film ($\mathbf{L}_{Sen}$) as a sensing material and to characterize the interactions between the Al(III) and the polymer structure (Scheme 2).

**Preparation and Characterization of the Sensory Materials.** The monomer containing the salicylaldehyde benzoylhydrazone sensory motif (**3**) was prepared in a straightforward manner from widely available commercial chemicals. First, hydrazine and ethyl 4-aminobenzoate were used, followed by two further reaction steps (as shown in Scheme 1). The overall yield was 40%. The NMR spectra of (**3**) obtained at rt is relatively simple (Figure S3, Supporting Information (SI)), and the assignment of all peaks via conventional NOESY and COSY experiments was straightforward (Figures S4 and S5, SI). However, heating the NMR sample revealed the more complex nature of (**3**) in the solution, and splitting the signals at a higher temperature indicated equilibria between the associated and nonassociated species (Figure 1), with a clear domination of the associated species at rt. In addition, unique $^{13}C$ NMR signals were observed for each nucleus. This feature was also observed in the $^{1}H$ NMR spectra (Figures S3–S5, SI).

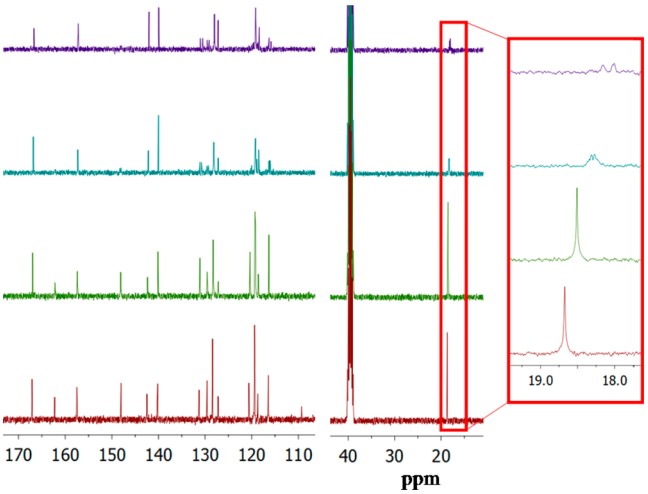


**Figure 1.** 100.58 MHz $^{13}C$ NMR spectra of monomer (**3**) in DMSO-$d_6$ at different temperatures (from top to bottom: 80, 60, 40, and 25 °C).

The sensory core is an excellent Al(III) chelator for different organic molecules in organic or aqueous/organic solutions.[24−29] Thus, we designed monomer (**3**) and prepared organic sensory materials to function in pure water. The conventional thermally initiated radical polymerization of (**3**) with the inexpensive commercial comonomers **VP** and **2HEA** resulted in the water-soluble linear copolymer ($\mathbf{L}_{Sen}$), and the addition of a cross-linker (**EGDMMA**) yielded the membrane ($\mathbf{M}_{Sem}$) (Scheme 2). Regarding the envisioned application, only approximately 1% of the synthetic sensory monomer (**3**) is needed for preparing the $\mathbf{L}_{Sen}$ and $\mathbf{M}_{Sem}$ as sensory materials. The $^{1}H$ NMR spectrum of $\mathbf{L}_{Sen}$ agrees with the feed monomer ratio of the polymerization reaction, including the small monomer (**3**) content, as depicted in Figure S11, SI.

The dense polymer membrane or film (see the surface and cross-section appearance in the SEM images, Figure S13, SI) was mechanically creasable and flexible, exhibiting a Young's modulus (MPa)/tensile strength (MPa)/elongation at breakage (%) under ambient conditions of 100/6/34. Drying the membranes at 60 °C for 30 min resulted in a significant increase in the Young's modulus and tensile strength, with a concomitant decrease in the elongation at break (394/31/23), demonstrating the influence of membrane hydration due to the humidity in the air.

Furthermore, the materials exhibited reasonably good thermal stability according to TGA. The decomposition temperature associated with a 10% weight loss under a nitrogen atmosphere was approximately 350 °C for both $\mathbf{L}_{Sen}$ and $\mathbf{M}_{Sem}$. However, the char yield at 800 °C was slightly higher for the cross-linked material (9% for $\mathbf{M}_{Sem}$ and 6% for $\mathbf{L}_{Sen}$). The TGA curves and full data are shown in Figure S12 in the SI. The material was designed to be hydrophilic to provide water solubility to the linear copolymer $\mathbf{L}_{Sen}$ and gel behavior of the membrane. The latter is a prerequisite because solvated Al(III) must enter the membrane to reach and interact with the receptor motifs. The water-swelling percentage (WSP) was 63% (between 40 and 100%), which is suitable for both the rapid diffusion of chemicals into the membrane and for maintaining tractability of the mechanical properties of the water-swelled materials.

**Depicting the Sensory Mechanism.** Salicylaldehyde benzoylhydrazone derivatives form complexes with Al(III) with published Al(III)/salicylaldehydate-derivative stoichiometries of 1:1[24] and 1:3.[25−29] Unlike organic ligands, these coordination complexes are highly fluorescent in solution. The stoichiometry of the published complexes remains unclear or are dependent on the salicylaldehyde derivative. Thus, we studied the complex stoichiometry to determine the sensory mechanism.

A complex ($\mathbf{C}_{1:3}$) was prepared by reacting $Al(NO_3)_3$ with (**3**) at a molar ratio of 1:3.

The $\mathbf{C}_{1:3}$ complex has a molecular weight of 994.00, and the analysis of its HR-ESI-MS spectrogram is coherent with the suggested stoichiometry of 1:3 (Figures S6 and S7, SI).

In the DMSO-$d_6$ solution, complex $\mathbf{C}_{1:3}$ reaches equilibrium with complex $\mathbf{C}_{1:2}$ (or $[Al(3)_2]^+$) and deprotonated (**3**) ($[(3)\text{-}H]^-$), $\mathbf{C}_{1:3} \rightleftharpoons \mathbf{C}_{1:2} + [(3)\text{-}H]^-$, as observed in the COSY experiments (Figures S8 and S9, SI).

This equilibrium was analyzed using $^{1}H$ NMR at different temperatures. At 30 °C, four peaks corresponding to the methyl groups were observed, one signal for the symmetric $\mathbf{C}_{1:3}$ complex, another signal for deprotonated $[(3)\text{-}H]^-$ and two signals for the nonsymmetric $\mathbf{C}_{1:2}$ complex. At 80 °C, two peaks corresponding to $\mathbf{C}_{1:2}$ were merged into one (Figure S8, SI).

Thus, the formation of the complex could be monitored using $^{27}Al$ NMR (Figure 2),[32] for which two main signals were obtained. The sharper signal at approximately 19 ppm corresponds to the symmetric $\mathbf{C}_{1:3}$ species, and the broader signal centered at approximately 16 ppm corresponds to the nonsymmetric $\mathbf{C}_{1:2}$ species. The small peak at approximately 5 ppm is derived from aluminum in the glass substrate of the reference material.

After analyzing the sensory mechanism ascribed to the formation of complexes with the monomer and Al(III), the same behavior is expected to be responsible for the sensing characteristics of the sensory polymer materials. Accordingly, we found evidence of the formation of complexes with an Al(III)/salicylaldehydate derivative with a stoichiometry of 1:3 in the Job's plot obtained from the fluorescence titration curves

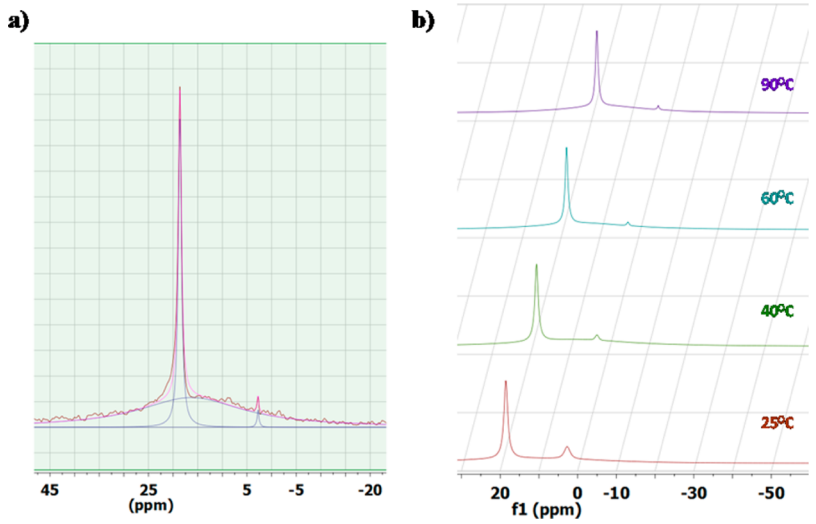


**Figure 2.** $^{27}$Al NMR spectra of $\mathbf{C}_{1:3}$: (a) curve fitting of the spectrum at 90 °C; (b) spectra at different temperatures. Solvent: DMSO-$d_6$/$D_2O$ (80:20).

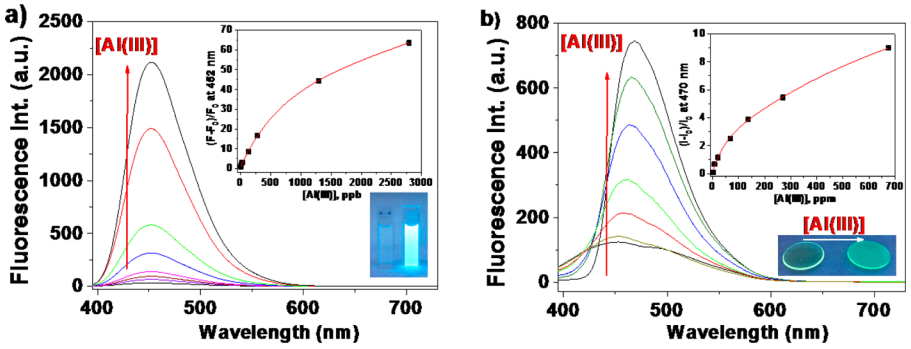


**Figure 3.** Titration of Al(III) in water using the fluorescence technique, (a) Fluorescence spectra of $\mathbf{L}_{Sen}$ in aqueous solution (inset) Al(III) concentration vs fluorescence enhancement; image captured under UV light, 364 nm. The $\mathbf{L}_{Sen}$ concentration was 2.81 g/L, corresponding to 0.25 mEq/L of the sensory motif (**3**). (b) The fluorescence spectra of the solid discs cut from $\mathbf{M}_{Sen}$ using 5 $\mu$L of water containing Al(III). (inset) Al(III) concentration vs fluorescence enhancement; image of sensory disc captured under UV light, 364. Conditions: Milli-Q water was buffered (NaOH/AcOH) at pH = 4.5; excitation slit = 5 nm; emission slit = 5 nm; excitation wavelength = 374 nm; scan speed = 12 000 nm/min; the Al(III) concentration was increased every 5 min in the $\mathbf{L}_{Sen}$ measurements; and in solid systems ($\mathbf{M}_{Sen}$), 5 $\mu$L of Milli-Q water containing different concentrations of Al(III) was placed on different discs, which were allowed to stand for 15 min before heating to 100 °C for an additional 5 min.

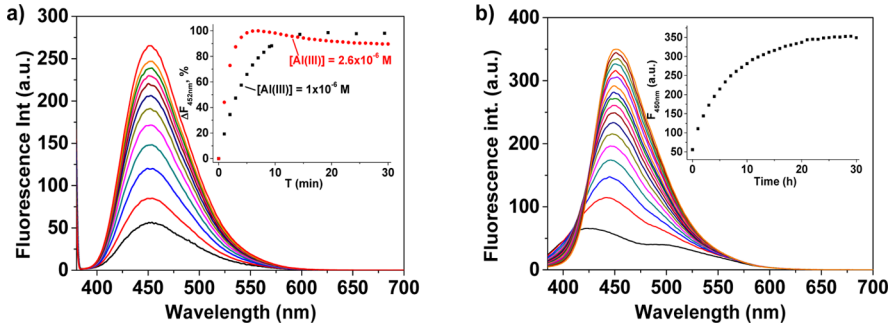


**Figure 4.** Response time experiments. Interactions of Al(III) in water (pH = 4.5, buffered with NaOH/AcOH) over time with $\mathbf{L}_{Sen}$ and $\mathbf{M}_{Sem}$. (a) The $\mathbf{L}_{Sen}$ in solution (the concentration of $\mathbf{L}_{Sen}$ was 2.81 g/L, corresponding to 0.25 mEq/L of the sensory motif (**3**)), the selected fluorescence spectra. (inset) Response in terms of the fluorescence intensity increase at 452 nm vs time. (b) The $\mathbf{M}_{Sem}$ immersed in a water solution containing Al(III) in a quartz cuvette. (inset) Response in terms of the fluorescence intensity at 450 nm vs time. Fluorescence spectra were recorded periodically. Conditions: water volume in cuvette = 2 mL; excitation slit = 5 nm; emission slit = 5 nm; excitation wavelength = 374 nm; scan speed = 12 000 nm/min; and [Al(III)] = 1 × $10^{-6}$ M (26.7 ppb). The response at a higher Al(III) concentration (2.6 × $10^{-4}$ M) was measured for $\mathbf{L}_{Sen}$ (inset, (a)) for comparative purposes.

of Al(III) with solutions of $\mathbf{L}_{Sen}$ in pure water. In this plot, a maximum was observed for a salicylaldehyde derivative molar fraction of 0.75 (Figure S10, SI).

**Sensing Behavior of the Sensory Materials.** As previously discussed, nonfluorescent pure aqueous solutions of $\mathbf{L}_{Sen}$ became highly fluorescent in the presence of aluminum


dx.doi.org/10.1021/am507458k | ACS Appl. Mater. Interfaces 2015, 7, 921−928

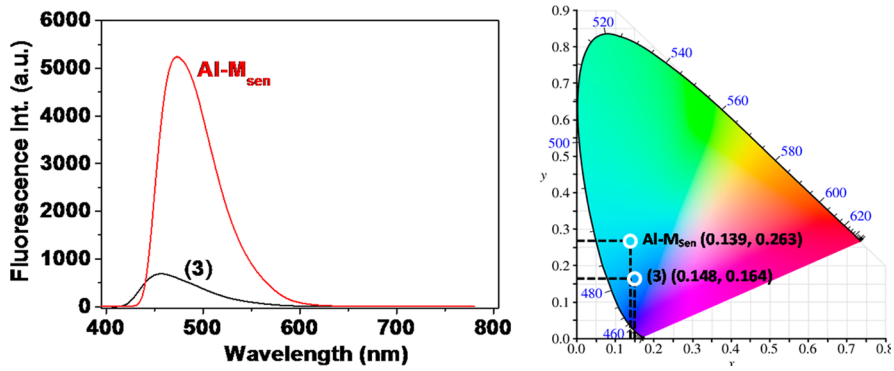


**Figure 5.** Fluorescence spectra (left) and the CIE chromaticity coordinates ($x$ and $y$) drawn on the CIE 1931 $xy$ chromaticity diagram (right, white ○) for the hybrid **Al-M$_{Sen}$** material. Measurement conditions: excitation slit = 5 nm; emission slit = 5 nm; excitation wavelength = 365 nm; scan speed = 12 000 nm/min; the CIE 1931 $xy$ chromaticity diagram is a public domain image downloaded from Wikipedia (http://commons.wikimedia.org/wiki/File:CIE1931xy_blank.svg).

ions (i.e., following an off−on pattern, as shown in Figure 3), which allowed us to draw a titration curve.

Following a similar off−on pattern, 5 mm discs cut from the **M$_{Sen}$** film resulted in a large increase in their fluorescence intensities upon immersion in water containing aluminum ions, as discussed below. In contrast, a manageable and highly fluorescent hybrid organic−inorganic film-shaped material (**Al-M$_{Sen}$**) was prepared after immersing **M$_{Sen}$** in a water solution of Al(III).

After preparing the sensory materials, critical parameters such as response time, interfering chemicals, selectivity, and sensitivity were measured, as discussed below. In addition, a short study of the performance of the hybrid film as a luminescent material was performed.

**Response Time.** The response time was significantly short (approximately 5 min) for the sensory system composed of an aqueous **L$_{Sen}$** solution at micromolar and millimolar Al(III) concentrations (Figure 4). The response time was not dependent on the Al(III) concentration.

However, the most interesting sensory solid system, **M$_{Sen}$**, showed a much longer response time, especially at a low Al(III) concentration. Moreover, this time was highly dependent on the Al(III) concentration. These trends were observed because the sensing phenomenon relies on two concomitant factors, namely, the relatively slow physical diffusion of the target species (Al(III)) into the membrane and the rapid chemical interactions of the species with the sensory motifs chemically anchored to the membrane polymer network. Thus, the response time for a submillimolar concentration of Al(III) was approximately 1 d, as shown in Figure 4.

Nevertheless, the response time of the **M$_{Sen}$** could be reduced to 20 min for the concentration of the target cation Al(III), achieving the goal of attaining a short measurement time. This reduction was accomplished by forcing the interaction to occur in the solid state (i.e., a known quantity of the aqueous solution containing Al(III) was dropped on the surface of a dry membrane disc and allowed to stand for 15 min, resulting in the immediate absorption of the Al(III) by the hydrophilic membrane structure, before drying the disc in an oven at 100 °C for 5 min). On one side, the rapid absorption of the aqueous drop by the membrane drags the solvated Al(III) ions into the material. On the other side, the simultaneous drying of the material forces the previously hydrated Al(III) ions to interact with the membrane sensory motifs (**3**).

**Hybrid Materials Al-M$_{Sen}$.** The addition of Al(III) to the DMA solutions of (**3**) caused the fluorescence to turn on, transforming the formerly weakly fluorescent solution into a highly fluorescent solution due to the formation of Al(**3**)$_n^{(3-n)+}$ complexes with Al(III)/(**3**) stoichiometries of 1:1, 1:2, and 1:3. The quantum yield of the solution containing (**3**) in DMA was negligible ($\Phi$ = 0.02) when using quinine sulfate in sulfuric acid (0.05 M) as a reference standard.[31] Furthermore, the addition of Al(III) to this solution at molar ratios of 1:1, 1:2, and 1:3 (with respect to (**3**)) resulted in quantum yields of $\Phi$ = 0.59, 0.53, and 0.59, respectively, indicating a high fluorescence efficiency, as previously outlined.

After determining that the high quantum yield of the organometallic complexes resulted from the interaction of (**3**) with Al(III), which was determined in organic media because (**3**) is water-insoluble, and based on the potential of the materials derived from (**3**) as luminescent converters (LUCO), the **Al-M$_{Sen}$** hybrid membrane was prepared (please see the SEM images in Figure S13 in the SI. The Al(III) content in the cross section of the membrane obtained from EDS analysis was 0.22%, which agreed well with the theoretical value of 0.20%). Furthermore, the color of the materials upon irradiation was determined in terms of the CIE chromaticity coordinates ($x$ and $y$) that were calculated from the fluorescence spectra using the corresponding CIE 1931 color matching functions (Figures 5).[33] Figure S13 in the SI contains an image of membrane **Al-M$_{Sen}$** strips under UV light. These types of materials are promising for luminescence conversion applications because of their high quantum yields and the blue emissions observed upon irradiation under conventional 365 nm UV. The CIE chromaticity coordinates were $x$ = 0.14 and $y$ = 0.26 for **Al-M$_{Sen}$** and were $x$ = 0.15 and $y$ = 0.16 for the monomer in the organic solution. Both systems showed blue emissions.

**Substrate Selectivity and Interference Study.** Preliminary interference studies regarding the sensory monomer (**3**) were conducted in organic/aqueous solutions due to the lack of the solubility of (**3**) in water. A broad set of cations was added to the sensing solutions at a high concentration (10 times the concentration of (**3**)), and only five cations significantly enhanced the fluorescence. A 24-fold enhancement occurred for Al(III) and 1- to 4-fold enhancements occurred for Zr(IV), Cd(II), Zn(II), and La(III), as shown in Table S1 in the SI. The greater response toward Al(III) was accompanied by a higher selectivity because the emission and excitation spectra are both characteristic of these cations, as shown in the 2D and


dx.doi.org/10.1021/am507458k | ACS Appl. Mater. Interfaces 2015, 7, 921−928

3D spectra (Figures S14–S19, SI). No fluorescence variations were observed after adding a broad set of anions.

An image captured under UV light (366 nm) clearly depicts the fluorescence "turn on" of the aforementioned cations (Figure S20, SI).

An interference study of $\mathbf{L}_{Sen}$ in pure aqueous solution depicted a different scenario. From a practical viewpoint, Zr(IV) is considered as a unique interferent. However, to test the performance of the sensory system, a competitive experiment was conducted (Figure 6). Thus, a cocktail of

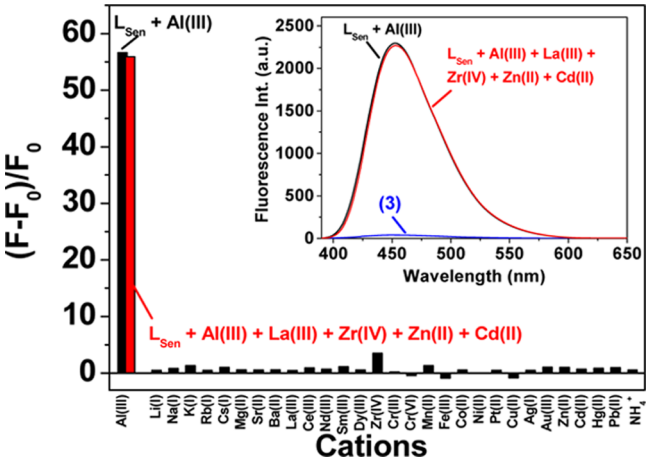


**Figure 6.** Fluorescence enhancement of an aqueous solution of $\mathbf{L}_{Sen}$ upon the addition of individual cations (black bars) and a cocktail of cations (red bar). (inset) Fluorescence spectra. Conditions: the concentration of the $\mathbf{L}_{Sen}$ was 2.81 g/L, corresponding to 0.25 mEq/L of the sensory motif (**3**); the concentration of each cation, both in the individual an in cocktail experiments, was $2.6 \times 10^{-4}$ M; the fluorescence intensity was measured at the maximum, 452 nm; excitation and emission slits = 5 nm; excitation wavelength = 374 nm; and scan speed = 12 000 nm/min.

cations was added to the solution, and the results were compared with those obtained from an experiment in which only Al(III) was added. The cocktail included the cations that caused interference to (**3**), and no significant effects due to these cations were observed regarding fluorescence enhancement and the fluorescence pattern, as shown in the inset of Figure 6. The same behavior was observed for the solid sensory substrate $\mathbf{M}_{Sen}$, in which the spectral patterns of the membrane with and without Al(III) differed from that of the solutions of (**3**) and $\mathbf{L}_{Sen}$ due to the solid swelled state, as illustrated in the 2D and 3D fluoresce spectra shown in Figures S21 and S22 (SI).

**Substrate Sensitivity.** Water solutions of $\mathbf{L}_{Sen}$ were used as off–on fluorescence probes for detecting Al(III) at concentrations ranging from 0.3 ppb to 2.8 ppm (Figure 4). The limit of detection (LOD) and the limit of quantification (LOQ)[34] were 1.5 and 4.7 ppb, respectively, below the Environmental Protection Agency (EPA) Secondary Drinking Water Regulation (SDWR, 50 to 2000 ppb).[35] In contrast, the LOD and LOQ achieved with the sensory disc cut from $\mathbf{M}_{Sen}$ were much higher, 22 and 36 ppm, respectively. Thus, the solution system presented the advantage of sensitivity, whereas the solid system provided the benefit of a short response time and simplicity.

## CONCLUSIONS

In summary, we designed an innovative solid material for the fluorescence off–on detection of Al(III). In addition, we developed a new method for measuring the concentration of Al(III) using one drop of the measuring solution that can be conducted within minutes and measure concentrations at the ppb level, which is significantly lower than the EPA-recommended concentrations for drinking water. The sensory material was a flexible polymer film that could be handled and exhibited gel behavior. The film was prepared using a novel fluorescence aluminum ion sensory salicylaldehyde benzoylhydrazone derivative and other comonomers to impart hydrophilicity and good mechanical properties. The measurement method consisted of depositing a drop of the solution to be measured onto the surface of the sensory film, which allowed it to enter the hydrophilic material. This process was followed by a drying period that forced the Al(III) to interact with the sensory motifs within the membrane. Overall, this process required approximately 20 min to complete. After this process, the fluorescence of the system was measured using conventional methods. In addition, a water-soluble sensory polymer using the sensory monomer was prepared, and its performance in detecting aluminum was characterized, which yielded results that were similar to those obtained for the films. However, the measurements involving solutions were much less labor-intensive and time-consuming.

## ASSOCIATED CONTENT

### Supporting Information

1D and 2D NMR and mass spectra of monomer (**3**) and complexation studies of (**3**) with Al(III). The $^1$H NMR spectra of $\mathbf{L}_{Sen}$, TGA of $\mathbf{L}_{Sen}$ and $\mathbf{M}_{Sen}$, SEM images of $\mathbf{M}_{Sen}$ and Al-$\mathbf{M}_{Sen}$, 2D and 3D fluorescence spectra of (**3**) and the $\mathbf{M}_{sen}$ with and without different cations in the media, and the interference study. This material is available free of charge via the Internet at http://pubs.acs.org.

## AUTHOR INFORMATION

### Corresponding Author

*Fax: (+) 34 947 258 831. Phone: (+) 34 947 258 085. E-mail: jmiguel@ubu.es.

### Notes

The authors declare no competing financial interest.

## ACKNOWLEDGMENTS

We gratefully acknowledge the financial support provided by the Spanish Ministerio de Economía y Competitividad-Feder (MAT2011-22544) and by the Consejería de Educación - Junta de Castilla y León (BU232U13).

## REFERENCES

(1) Álvarez, E.; Fernández-Marcos, M. L.; Monterroso, C.; Fernández-Sanjurjo, M. J. Application of Aluminium Toxicity Indices to Soils under Various Forest Species. *For. Ecol. Manage.* **2005**, *211*, 227–239.

(2) Barceló, J.; Poschenrieder, C. Fast Root Growth Responses, Root Exudates, and Internal Detoxification as Clues to the Mechanisms of Aluminium Toxicity and Resistance: a Review. *Environ. Exp. Bot.* **2002**, *48*, 75–92.

(3) Alstad, N. E. W.; Kjelsberg, B. M.; Vøllestad, L. A.; Lydersen, E.; Poléo, A. B. S. The Significance of Water Ionic Strength on Aluminium Toxicity in Brown Trout (Salmo Trutta L.). *Environ. Pollut.* **2005**, *133*, 333–342.

(4) Cronan, C. S.; Walker, W. J.; Bloom, P. R. Predicting Aqueous Aluminium Concentrations in Natural Waters. *Nature* **1986**, *324*, 140−143.
(5) Nayak, P. Aluminum: Impacts and Disease. *Environ. Res.* **2002**, *89*, 101−115.
(6) Fasman, G. D. Aluminum and Alzheimer's Disease: Model Studies. *Coord. Chem. Rev.* **1996**, *149*, 125−165.
(7) Berthon, G. Aluminium Speciation in Relation to Aluminium Bioavailability, Metabolism and Toxicity. *Coord. Chem. Rev.* **2002**, *228*, 319−341.
(8) Pierides, A. M.; Edwards, W. G., Jr.; Cullum, U. X., Jr.; McCall, J. T.; Ellis, H. A. Hemodialysis Encephalopathy with Osteomalacic Fractures and Muscle Weakness. *Kidney Int.* **1980**, *18*, 115−124.
(9) Alfrey, A. C. Aluminum. *Adv. Clin. Chem.* **1983**, *23*, 69−91.
(10) Perl, D. P.; Gajdusek, D. C.; Garruto, R. M.; Yanagihara, R. T.; Gibbs, C. J. Intraneuronal Aluminum Accumulation in Amyotrophic Lateral Sclerosis and Parkinsonism-Dementia of Guam. *Science* **1982**, *217*, 1053−1055.
(11) Perl, D. P.; Brody, A. R. Alzheimer's Disease: X-ray Spectrometric Evidence of Aluminum Accumulation in Neurofibrillary Tangle-Bearing Neurons. *Science* **1980**, *208*, 297−299.
(12) El-Sayed, W. M.; Al-Kahtani, M. A.; Abdel-Moneim, A. M. Prophylactic and Therapeutic Effects of Taurine Against Aluminum-Induced Acute Hepatotoxicity in Mice. *J. Hazard. Mater.* **2011**, *192*, 880−886.
(13) Shokrollahi, A.; Ghaedi, M.; Niband, M. S.; Rajabi, H. R. Selective and Sensitive Spectrophotometric Method for Determination of Sub-Micro-Molar Amounts of Aluminium Ion. *J. Hazard. Mater.* **2008**, *151*, 642−648.
(14) Kepp, K. P. Bioinorganic Chemistry of Alzheimer's Disease. *Chem. Rev.* **2012**, *112*, 5193−5239.
(15) Park, H. M.; Oh, B. N.; Kim, J. H.; Qiong, W.; Hwang, I. H.; Jung, K.-D.; Kim, C.; Kim, J. Fluorescent Chemosensor Based-on Naphthol−Quinoline for Selective Detection of Aluminum Ions. *Tetrahedron Lett.* **2011**, *52*, 5581−5584.
(16) Kim, S. H.; Choi, H. S.; Kim, J.; Joong, S.; Quang, D. T.; Kim, J. S. Novel Optical/Electrochemical Selective 1,2,3-triazole Ring-Appended Chemosensor for the $Al^{3+}$ Ion. *Org. Lett.* **2010**, *12*, 560−563.
(17) Maity, D.; Govindaraju, T. Pyrrolidine Constrained Bipyridyl-Dansyl Click Fluoroionophore as Selective $Al^{3+}$ Sensor. *Chem. Commun.* **2010**, *46*, 4499−4501.
(18) Cheng, X.-Y.; Wang, M.-F.; Yang, Z.-Y.; Li, Y.; Li, T.-R.; Liu, C.-J.; Zhou, Q.-X. A Highly Sensitive and Selective Schiff Base Fluorescent Chemodosimeter for Aluminum(III). *J. Coord. Chem.* **2013**, *66*, 1847−1853.
(19) Lee, J.; Kim, H.; Kim, S.; Noh, J. Y.; Song, E. J.; Kim, C.; Kim, J. Fluorescent Dye Containing Phenol-Pyridyl for Selective Detection of Aluminum Ions. *Dyes Pigm.* **2013**, *96*, 590−594.
(20) Liao, Z.-C.; Yang, Z.-Y.; Li, Y.; Wang, B.-D.; Zhou, Q.-X. A Simple Structure Fluorescent Chemosensor for High Selectivity and Sensitivity of Aluminum Ions. *Dyes Pigm.* **2013**, *97*, 124−128.
(21) Wang, Y.-W.; Yu, M.-X.; Yu, Y.-H.; Bai, Z.-P.; Shen, Z.; Li, F.-Y.; You, X.-Z. A Colorimetric and Fluorescent Turn-On Chemosensor for $Al^{3+}$ and its Application in Bioimaging. *Tetrahedron Lett.* **2009**, *50*, 6169−6172.
(22) Maity, S. B.; Bharadwaj, P. K. A Chemosensor Built with Rhodamine Derivatives Appended to an Aromatic Platform via 1,2,3-Triazoles: Dual Detection of Aluminum(III) and Fluoride/Acetate Ions. *Inorg. Chem.* **2013**, *52*, 1161−1163.
(23) Ma, T.-H.; Dong, M.; Dong, Y.-M.; Wang, Y.-W.; Peng, Y. A Unique Water-Tuning Dual-Channel Fluorescence-Enhanced Sensor for Aluminum Ions Based on a Hybrid Ligand from a 1,1′-Binaphthyl Scaffold and an Amino Acid. *Chem.—Eur. J.* **2010**, *16*, 10313−10318.
(24) Tiwari, K.; Mishra, M.; Singh, V. P. A Highly Sensitive and Selective Fluorescent Sensor for $Al^{3+}$ Ions Based on Thiophene-2-carboxylic Acid Hydrazide Schiff Base. *RSC Adv.* **2013**, *3*, 12124−12132.
(25) Jiang, C.; Tang, B.; Wang, C.; Zhang, X. Spectrofluorimetric Determination of Trace Amounts of Aluminium with Salicylaldehyde Salicyloylhydrazone. *Analyst* **1996**, *121*, 317−320.
(26) Mánuel-Vez, M. P.; García-Vargas, M. Fluorimetric Determination Traces of Aluminium in Soil Extracts. *Talanta* **1994**, *41*, 1553−1559.
(27) Jiang, C.; Tang, B.; Wang, R.; Cheng, J. Spectrofluorimetric Determination of Trace Amounts of Aluminium with 5-Bromo-salicylaldehyde Salicyloylhydrazone. *Talanta* **1997**, *44*, 197−202.
(28) Suryawanshi, V. D.; Gore, A. H.; Dongare, P. R.; Anbhule, P. V.; Patil, S. R.; Kolekar, G. B. A Novel Pyrimidine Derivative as a Fluorescent Chemosensor for Highly Selective Detection of Aluminum (III) in Aqueous Media. *Spectrochim. Acta, Part A* **2013**, *114*, 681−686.
(29) Guo, Y.-Y.; Yang, L.-Z.; Ru, J.-X.; Yao, X.; Wu, J.; Dou, W.; Qin, W.-W.; Zhang, G.-L.; Tang, X.-L.; Liu, W.-S. An "OFF−ON" Fluorescent Chemosensor for Highly Selective and Sensitive Detection of Al (III) in Aqueous Solution. *Dyes Pigm.* **2013**, *99*, 693−698.
(30) Vallejos, S.; Muñoz, A.; Ibeas, S.; Serna, F.; García, F. C.; García, J. M. Selective and Sensitive Detection of Aluminium Ions in Water Via Fluorescence "Turn-On" with both Solid and Water Soluble Sensory Polymer Substrates. *J. Hazard. Mater.* **2014**, *276*, 52−57.
(31) Brouwer, A. M. Standards for Photoluminescence Quantum Yield Measurements in Solution (IUPAC Technical Report). *Pure Appl. Chem.* **2011**, *83*, 2213−2228.
(32) Tashiro, M.; Furihata, K.; Fujimoto, T.; Machinami, T.; Yoshimura, E. Characterization of the Malate-Aluminum(III) Complex Using $^{1}H$ and $^{27}Al$ NMR Spectroscopy. *Magn. Reson. Chem.* **2007**, *45*, 518−521.
(33) International Commission on Illumination (http://cie.co.at/). The color matching parameters were downloaded for free from the CIE web page (http://files.cie.co.at/204.xls). Access date: November 8, 2013.
(34) The limit of detection (LOD) and the limit of quantification (LOQ) were calculated from the titration curves using the following equations: LOD = 3.3x*SD*/*s* and LOQ = 10x*SD*/*s*, where SD is the standard deviation of the blank sample, and *s* is the slope of the calibration curve in a region with low analyte content.
(35) The U.S. Environmental Protection Agency (EPA) has established a limit of 50 to 200 ppb for aluminum in drinking water (non-enforceable guidelines regarding cosmetic or aesthetic effects). Source: 2012 Edition of the Drinking Water Standards and Health Advisories, EPA 822-S-12−001, http://water.epa.gov/action/advisories/drinking/upload/ dwstandards2012.pdf, accessed October 20, 2014.